Carbohydrate Polymers 94 (2013) 468–478

Contents lists available at SciVerse ScienceDirect

Carbohydrate Polymers

journal homepage: www.elsevier.com/locate/carbpol

Correlations between steric/thermochemical parameters and *O*-/*N*-acylation reactions of cellulose☆

Kesavan Devarayan[a], Taketoshi Hayashi[a], Masakazu Hachisu[b], Jun Araki[c], Kousaku Ohkawa[a,*]

[a] *Institute of High Polymer Research, Faculty of Textile Science and Technology, Shinshu University, Tokida 3-15-1, Ueda 386-8567, Japan*
[b] *Research Institute of Genome-based Biofactory, National Institute of Advanced Industrial Science and Technology (AIST), 2-17-2-1, Tsukisamu-higashi, Toyohira-ku, Sapporo 062-8517, Japan*
[c] *Functional Polymer Science Course, Division of Chemistry and Materials, Faculty of Textile Science and Technology, Shinshu University, Tokida 3-15-1, Ueda 386-8567, Japan*

ARTICLE INFO

Article history:
Received 11 September 2012
Received in revised form
29 November 2012
Accepted 31 December 2012
Available online 16 January 2013

Keywords:
Conjugated polymers
Cellulose
Molecular modeling
Peptides
Synthesis

ABSTRACT

N^{α}-*t*-Butyloxycarbonyl (Boc)-amino acids (X_{aa} = Gly, Ala, or β-Ala) were reacted with the cellulose hydroxyl groups (*O*-acylation) using *N*,*N*′-carbonyl diimidazole. The degrees of substitution toward the total hydroxyl groups (DS%(/OH)s) were 38% for *O*-(Boc-Gly)-Cellulose, 29% for *O*-(Boc-Ala)-Cellulose and 53% for *O*-(Boc-β-Ala)-Cellulose. The one-by-one *N*-acylation between the *O*-(X_{aa})-Celluloses and Boc-Ala-Gly using a water-soluble carbodiimide yielded the conjugates *N*-(Boc-Ala-Gly)-X_{aa}-Celluloses with DS%(/NH_2) values of 25% (X_{aa} = Gly), 35% (Ala), and 48% (β-Ala), respectively. The results were well correlated with ΔG and ΔE_{strain} profiles, which were predicted by semi-empirical thermochemical parameter calculation coupled with conformer search ($R^2 > 0.90$). *N*-Acylation of the *O*-(β-Ala)-Cellulose using various length of oligo-peptides, Boc-(Ala-Gly)$_n$ and Boc-(Gly-Ala)$_n$ (where, n = 0.5, 1.0, 1.5, 2.0, 3.0), suggested that the DS%(/NH_2) was dependent on the structural features of the symmetric anhydrides as the *N*-acylating agents, including conformer populations and their transition energy.

1. Introduction

Chemical modifications of cellulose have been investigated for a long time, and the ideas for utilizations of natural amino acids are still diverse, including a broad spectrum for applications of the cellulose–amino acids conjugated molecules (Heinze & Liebert, 2001). One of the earliest reports on the amino acid-modified cellulose derivatives has already adopted two major principles (Gardner, 1946), *i.e.*, one is conjugation of the α-amino group to the chemically derivatized cellulose, which typically employs the carboxymethyl functionalities (Sun, Derevitskaya, & Rogovin, 1959), which has been later applied to other carboxylated co-polymers (Luo, Stewart, Hirt, Husson, & Schwark, 2004). Diisocyanates also mediate the conjugation between the α-NH_2 of certain amino acid esters and the hydroxyl groups on the intact cellulose molecules, and subsequent removal of the ester group yields the carboxylated cellulose derivatives (Sato, Karatsu, Kitamura, & Ohno, 1983). These approaches are the so-called "*N*-end-on synthesis."

Other strategies are similar to the cellulose ester preparation using the carboxylic acids and the carboxyl group-activating agents (Liebert & Heinze, 2005), which enables the nucleophilic attack by the cellulose hydroxyls. The *O*-acylation of cellulose using the *N*-protected amino acids can then be referred to as the "*C*-end-on synthesis," of which the earliest application was directed to immobilize the amino acids onto an insoluble cellulose-seat surface, where the oligopeptide chains were elongated in a stepwise manner often used for solid-phase peptide synthesis (Frank & Doring, 1988). This method was designated as the "spot-synthesis," and at present, developed as the one of the most successful strategies to construct peptide libraries on the cellulose-seat surfaces (Adler, Frank, Lanzavecchia, & Weiss, 1994). The dimer of β-alanine (β-Ala) and N^{β}-9-fluorenylmethyloxycarbonyl-β-Ala were found as fairly useful carriers (or linkers) for the N^{α}-protected first residue to be bound onto the modified cellulose seat (Kramer et al., 1999; Winkler, 2011).

The *C*-end-on approach can also be applied to the preparation of the amino-functionalized cellulose in homogenous solution reaction systems *via* ring-opening reactions, *e.g.*, using 2.0 equiv.mol or more excess amount of C4–C6 lactams toward anhydroglucopyranose units (D-Glc), which yielded several kinds of primary amino- or *N*-methyl-amino groups-containing cellulose esters having the degree of substitution as DS = 0.24–1.17 per D-Glc (Zarth, Koschella, Pfeifer, Dorn, & Heinze, 2011). In our previous studies, the *O*-(β-Ala)-Cellulose was prepared *via* the *N*,*N*'-carbonyl diimidazole-mediated *O*-acylation of the parent cellulose in a

☆ Part 3 of a series: Synthesis of soluble cellulose derivatives having β-Ala esters.
* Corresponding author. Tel.: +81 268 215573; fax: +81 268 215571.
E-mail address: kohkawa@shinshu-u.ac.jp (K. Ohkawa).

0144-8617/$ – see front matter © 2013 Elsevier Ltd. All rights reserved.
http://dx.doi.org/10.1016/j.carbpol.2012.12.074

homogenous solution using 1.67 equiv.mol OH (5.0 equiv.mol of D-Glc) of N^{β}-Boc-β-Ala, and the subsequent removal of Boc produced the *O*-(β-Ala)-Cellulose, of which the DS values were 1.44–1.50 per D-Glc (Ohkawa, Nishibayashi, Devarayan, Hachisu, & Araki, 2013).

The *O*-(β-Ala)-Cellulose was soluble in water and also in several organic solvents. The *N*-acylation of *O*-(β-Ala)-Cellulose enables the synthesis of more complex conjugate molecules, indicating that the *O*-(β-Ala)-Cellulose is a useful intermediate for the multi-purpose functionalization of cellulose, which involves a two-step chemical modification; first, *O*-acylation using Boc-β-Ala followed by regeneration of the β-amino groups, and second, *N*-acylation of *O*-(β-Ala)-Cellulose using the pre-assembled *N*-protected oligopeptides having a free α-COOH at the *C*-end residues, and subsequent deprotection of the conjugated peptides. The latter step allowed the successful syntheses of the adhesive peptides (Ohkawa et al., 2013) and the phosphorylated peptides (Devarayan, Hachisu, Araki, & Ohkawa, 2013)–*O*-(β-Ala)-Cellulose conjugates, as suppressing the amount of the pre-assembled protected oligopeptides to be lost unreacted. The high efficiencies for the *N*-substitutions of the *O*-(β-Ala)-Cellulose are rather profitable, since usually, the pre-assembling of the protected peptides is achieved *via* multiple steps of the chain elongation of the peptide backbones, as well as the requirements as the careful protection strategies for the side chain functionalities, and the time- and/or cost-consuming repetitive coupling and purification procedures for each of the intermediate compounds (Devarayan et al., 2013; Yamamoto, Saitoh, & Ohkawa, 2003).

If the conjugate components are restricted to the cellulose and the amino acids of natural occurrence, then a fundamental issue has occurred; the reason why the profitable property originates with the β-amino acid for binding the pre-assembled peptides. The present study was undertaken to understand and explain this issue, based on the following experiments: (i) comparisons of *N*-protected α,L- and β-amino acids (Boc-X_{aa}, X_{aa} = Gly, α,L-Ala, and β-Ala) for the *O*-acylation reaction of the parent cellulose in homogenous solutions, (ii) examination on the *N*-acylation of the X_{aa}-Cellulose esters using a simple dipeptide, Boc-Ala-Gly, and (iii) *N*-acylation of the β-Ala-Cellulose using various lengths of the oligo-peptides having dipeptide repeat units, Boc-(Ala-Gly)$_n$ and Boc-(Gly-Ala)$_n$ (n = 0.5, 1.0, 1.5, 2.0, and 3.0).

More recently, various aspects on the polymer chemical properties of cellulose and its derivatives have been analyzed by means of computational methods, including swelling behavior of the cellulose I_{β} crystal model (Yui, Nishimura, Akiba, & Hayashi, 2006), gas phase conformations of the cellulose oligomers (Queyroy, Muller-Plathe, & Brown, 2004), enzymatic degradability of the cellulose esters (Yoshida, Isogai, & Tsujii, 2008), adsorption of xylans on the cellulose surface (Mazeau & Charlier, 2012), dissolution process of the cellulose triacetate in organic solvent (Hayakawa, Ueda, Yamane, Miyamoto, & Horii, 2011), and so on. The present results on the degrees of the *O*- and *N*-acylations were characterized based on the steric and thermochemical parameters, which were estimated using the cellotetraose-derived molecular modelings and the computer-based conformer search/thermochemical calculations.

2. Materials and methods

2.1. Materials

Triethylamine (TEA), trifluoroacetic acid (TFA), dicyclohexyl carbodiimide (DCCI), 1-ethyl-3-(3-dimethylaminopropyl) carbodiimide monohydrochloride (EDC), di-*tert*-butyldicarbonate [$(Boc)_2O$], thioanisole, dimethyl formamide (DMF), anhydrous dimethylsulfoxide (DMSO, water < 50 ppm), anhydrous dimethyl acetamide (DMAc), lithium chloride (LiCl), 25% hydrogen bromide in acetic acid (HBr/AcOH), and isobutyl chloroformate (IBCF) were purchased from the Wako Pure Chemical Industries, Ltd; a commercial cellulose preparation (from cotton) was from Sigma–Aldrich, Japan. All of the protected peptides, Boc-(Ala-Gly)$_n$ and Boc-(Gly-Ala)$_n$, were synthesized as described in "Supplementary Data."

2.2. Cellulose-N-Boc-amino acid esters

Cellulose (1.00 g, 6.20 mmol D-Glc residues) was repeatedly shaken at 24-h intervals in distilled water at room temperature, and then the distilled water was removed by filtration. The solvent was replaced with acetone, followed by anhydrous DMAc, and the cellulose was finally added in DMAc/LiCl (LiCl, 8.0 wt.%) and stirred for 9 days to obtain a homogenous solution (Yanagisawa, Shibata, & Isogai, 2004).

The molar stoichiometry between the hydroxyl groups on the D-glucopyranose residues (D-Glc) of cellulose and the α-carboxyl groups of the Boc-X_{aa} (X_{aa} = Gly, Ala, β-Ala) were fixed at a 1.67 molar excess (equiv.mol/OH), which means that the *N*-Boc-X_{aa} was in 5.0 molar excess with respect to the D-Glc units, the reaction condition of which has been optimized in a previous report, including solvent and stoichiometry, for the maximum-yield efficiency within 1.0% of the degree of substitution reproducibility (Ohkawa et al., 2013). Boc-Gly (2.71 g, 15.5 mmol), Boc-L,α-Ala (Ala; 2.92 g, 15.5 mmol), or Boc-β-Ala (2.92 g, 15.5 mmol) was dissolved in anhydrous DMAc (8 mL), and then mixed with CDI (2.51 g, 15.5 mmol) in anhydrous DMAc (8 mL). The evolution of CO_2 immediately occurred, and after 10 min, the solution was incubated at 60 °C for 24 h with stirring. This mixture was combined with the cellulose/DMAc/LiCl solution (9.27 mmol OH in total cellulose) and the reaction was continued at 60 °C for 24 h.

The reaction mixture was added dropwise to aqueous 5% $NaHCO_3$ (800 mL) to remove the unreacted Boc-X_{aa} and a subproduct, imidazole. The product was aggregated in a powder and recovered by filtration. The crude product was washed in distilled water (500 mL) for 1 h with stirring and filtered, followed by lyophilization for recovery. The crude product was dissolved in DMSO (30 mL) and the solution was added dropwise to distilled water (400 mL) for purification by means of re-precipitation. After stirring for 1.5 h, the precipitates were filtered, washed with distilled water, and finally lyophilized. The three kinds of the products were designated as *O*-(Boc-Gly)-Cellulose, *O*-(Boc-Ala)-Cellulose, and *O*-(Boc-β-Ala)-Cellulose.

2.3. Elemental analysis

The elemental analysis (carbon, hydrogen, and nitrogen) was performed using a Yanagimoto CHN corder MT3, and the samples, *O*-(Boc-Gly)-Cellulose, *O*-(Boc-Ala)-Cellulose, and *O*-(Boc-β-Ala)-Cellulose (ca. 2.0–2.5 mg). The detected nitrogen element in μmol was equal to the Boc-amino acid (Boc-X_{aa}) content in mol per normalized sample weight, because the parent cellulose does not contain nitrogen element. The nitrogen content values were calculated as the DS%(/OH), according to our previous studies (Devarayan et al., 2013).

2.4. Deprotection of cellulose-O-(Boc-X_{aa}) esters

O-(Boc-Gly)-Cellulose, *O*-(Boc-Ala)-Cellulose, or *O*-(Boc-β-Ala)-Cellulose (each 0.5 g) was dissolved in TFA (6 mL) on ice bath and stirred for 3 h under a dry atmosphere. Absolute diethyl ether (distilled from sodium) was poured into the reaction mixture to precipitate the products, *O*-(X_{aa})-Cellulose TFA salts. The product was filtered, repeatedly washed with diethyl ether, and then dried *in vacuo*.

2.5. N-Acylation of O-(X_{aa})-Cellulose using Boc-Ala-Gly

The *N*-selective acylation of *O*-(X_{aa})-Cellulose using Boc-Ala-Gly was performed with EDC as previously reported (Ohkawa et al., 2013). As an example for the *N*-acylation of *O*-(Gly)-Cellulose, EDC (0.12 g, 0.65 mmol, 1.1 equiv.mol/NH_2) was added to the DMSO solution of Boc-Ala-Gly (5 mL). TEA (82 μL, 0.59 mmol, 1.0 equiv.mol/NH_2) was dispensed to the *O*-(Gly)-Cellulose TFA salt (0.25 g, 0.59 mmol Gly) in the DMSO solution (5 mL), and then the mixture was immediately combined with the EDC-activated Boc-Ala-Gly. The conjugation reaction was continued for 24 h, and then the unreacted materials and sub-products were removed by dialysis against distilled water (molecular weight cut-off; 3500). The dialysate was lyophilized to recover the crude product powder of *N*-(Boc-Ala-Gly)-Gly-Cellulose, and the powder was dispersed in methanol for washing, followed by recovery by filtration and then dried *in vacuo*. By using *O*-(Ala)-Cellulose and *O*-(β-Ala)-Cellulose, the similar conjugation reaction yielded *N*-(Boc-Ala-Gly)-Ala-Cellulose (purified by washing with ethyl acetate) and *N*-(Boc-Ala-Gly)-β-Ala-Cellulose (purified by washing with ethanol), respectively.

2.6. Direct conjugation of Boc-Ala-Gly with intact cellulose

CDI (1.65 g, 10.2 mmol) was added to the Boc-Ala-Gly (2.28 g, 9.24 mmol) dissolved in DMSO (16 mL) and the reaction mixture was stirred at 60 °C for 24 h. The cellulose (3.08 mmol D-Glc) solution was prepared *via* solvent replacement method and combined with the pre-activated Boc-Ala-Gly, and the *O*-acylation reaction was continued for 24 h at 60 °C. The recovery and purification (by washing with diethyl ether) of the product, *O*-(Boc-Ala-Gly)-Cellulose, was performed as described above.

2.7. Amino acid composition analysis

N-(Boc-Ala-Gly)-Gly-Cellulose, *N*-(Boc-Ala-Gly)-Ala-Cellulose, *N*-(Boc-Ala-Gly)-β-Ala-Cellulose, and *O*-(Boc-Ala-Gly)-Cellulose (each ca. 2–3 mg) were subjected to complete hydrolysis using 250 μL of 6 N HCl at 110 °C for 24 h in vacuum-sealed tubes (Kuboe, Tonegawa, Ohkawa, & Yamamoto, 2004; Tonegawa et al., 2004). The hydrolysates were dried-up and diluted in an acidic citrate buffer (pH 2.2) (Wako Pure Chemical Ind., Osaka, Japan). The amino acid compositions in the samples were performed using a Shimadzu LCVp10 amino acid composition analyzer system (Ohkawa, Nishida, Yamamoto, & Waite, 2004). The molar ratios between Ala, Gly, and β-Ala gave the DS%(/NH_2) values (Devarayan et al., 2013; Ohkawa et al., 2013).

2.8. N-Acylation of β-Ala-Cellulose using various Boc-peptides

As routine procedures, *O*-(β-Ala)-Cellulose TFA salt (DS%(/OH) = 53%, ca. 0.1–0.5 g) was treated with Boc-$(Ala\text{-}Gly)_n$ and Boc-$(Gly\text{-}Ala)_n$ (n = 0.5, 1.0, 1.5, 2.0, and 3.0) using the similar procedure described under Section 2.5. The molar stoichiometry between the materials to be conjugated and the primary amino groups on the *O*-(β-Ala)-Cellulose was varied at 1.0 and 4.0 equiv.mol NH_2. The DS%(/NH_2) values were determined by the amino acid composition analysis as previously described. After the conjugation reaction, a portion of each product was subjected to removal of the Boc to yield the TFA salt of the conjugate, which was used in the following solubility tests.

2.9. Solubility tests

The samples (2.0 mg) were placed in small tubes (volume, 600 μL) with 100 μL of solvents, including distilled water, methanol, acetone, chloroform, 1,4-dioxane, benzene, and DMSO. After vigorous shaking for 10 min, the samples were centrifuged (8100 × *g* for 15 min at room temperature). The qualitative solubility was represented as follows: S, soluble (no precipitate visually observed after centrifugation); SW, swollen (solvated transparent or translucent particles left); IS, insoluble (solid particles or opaque materials left).

2.10. CONFLEX™/MMFF94s-based conformer search

Three kinds of simplified models for the *O*-(Boc-X_{aa})-Cellulose esters were constructed (Hanwell et al., 2012) as a randomly substituted molecule; *i.e.*, methyl 4-*O*-methyl-β-D-glucopyranosyl-(1 → 4)-2-*O*-(Boc-X_{aa})-β-D-glucopyranosyl-(1 → 4)-3-*O*-(Boc-X_{aa})-β-D-glucopyranosyl-(1→4)-6-*O*-(Boc-X_{aa})-β-D-glucopyranoside (X_{aa} = Gly, Ala, or β-Ala), the backbones of which corresponded to a cellotetraose having both the -1- and -4- ends methylated. The models, therefore, were designated as "*O*-(Boc-X_{aa})-cellotetraoses." The model conformers of the lowest steric energy values (E_{steric}, kcal/mol) were generated in the gas phase using CONFLEX versions 6.8.3 and 7A softwares (Conflex Co., Ltd., Tokyo, Japan) (Goto & Osawa, 1989, 1993) (force field, MMFF94s (Halgren, 1999); steric energy (E_{steric}) search limit, 3.0 kcal/mol) for pre-search, then 3.0 kcal/mol for chemically significant convergence. Because the direct comparison of the E_{steric} values among the non-conformational isomers is prohibited, the strain energy values (Burkert & Allinger, 1982), which were obtained from the geometry optimization output files of the same softwares, were concerned as follows:

$$E_{strain} = E_{bond} + E_{angle} + E_{torsion} + E_{op\text{-}angle} + E_{nonbond} \quad (1)$$

where each of subscript symbols denotes the strain energy (E_{strain}, kcal/mol) as the sum of total bond, angle, torsion, out-of-plane angle, and non-bonded strain energies, respectively. The conformer distributions (conformer population: CP, %) were also taken into account for the semi-quantitative characterization of the cellulose-*O*-acylation reactions using Boc-X_{aa}s. The Boc-free models were similarly evaluated for the *N*-acylation reactions of the X_{aa}-Cellulose esters using Boc-Ala-Gly, in which the simplified models were described as "*N*-(Boc-Ala-Gly)-X_{aa}-cellotetraoses."

2.11. Thermochemical calculations

The conformer populations of the above parent and product cellotetraose derivatives and also the *O*-/*N*-acylating agents were subjected to the Gaussian09-based thermochemical parameter determination (Frisch et al., 2009), using a semi-empirical Hamiltonian parameter set, PM6 (Stewart, 2007), under standard conditions (298.15 K and 1.0 atm). Enthalpy (*H*, kcal/mol), entropy (*S*, cal/K mol), and Gibbs's free energy (*G*, kcal/mol) values were employed to evaluate the free energy transitions (ΔG, kcal/mol) in the *O*-/*N*-acylation of the cellulose derivatives in order to discuss the observed DS%(/OH) and DS%(/NH_2) results, with concerning the strain energy (ΔE_{strain}, kcal/mol) values of the chemical species. The evaluation procedures are described in the following sections.

3. Results and discussion

3.1. O-(Boc-X_{aa})-Cellulose esters

The DS%(/OH) values were 38% for *O*-(Boc-Gly)-Cellulose, 29% for *O*-(Boc-Ala)-Cellulose, and 53% for *O*-(Boc-β-Ala)-Cellulose, indicating that Boc-β-Ala was most effectively introduced to the

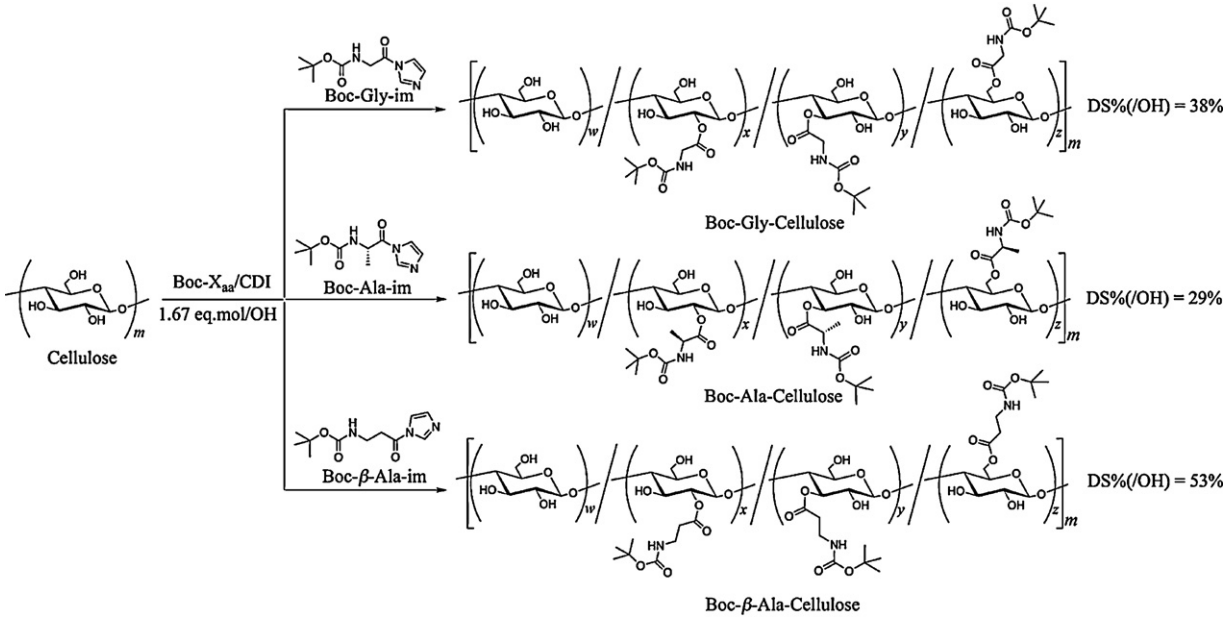

Scheme 1. Synthesis of Boc-X$_{aa}$-Celluloses *via* CDI-mediated *O*-acylation reactions.

cellulose hydroxyls (Scheme 1). The *O*-acylation reaction was represented as the following chemical transition model:

$$m\ \text{Boc-X}_{aa}\text{-im} + \text{cellotetraose} \rightarrow \textit{O}\text{-}(m\,\text{Boc-X}_{aa})\text{-cellotetraose} + m\,\text{imidazole} \quad (2)$$

where the *O*-acylating agents, Boc-X$_{aa}$-ims, represent the imidazole condensates of the Boc-X$_{aa}$s (Scheme 1). The stoichiometry numbers were set in $m = 3$ for a randomly (*O*-6, *O*′-3, *O*″-2)-tri-acylated model as described previsouly (Devarayan et al., 2013) and also in $m = 12$ for the totally *O*-acylated model, of which the Gibbs's energy transitions were weighted with the observed DS%(/OH) in order to estimate the in-reaction values as given below:

$$\Delta G^{Tri} = G_f^{Tri} - G_i^{Tri} \quad \text{for } m = 3 \quad (3)$$

$$\Delta G_e^{Tri} = \Delta G^{Tri} \times (DS\%(/\text{OH})/100) \quad \text{for } m = 3 \quad (4)$$

and

$$\Delta G^{TA} = G_f^{TA} - G_i^{TA} \quad \text{for } m = 12 \quad (5)$$

$$\Delta G_e^{TA} = \Delta G^{TA} \times (\text{DS\%}(/\text{OH})/100) \quad \text{for } m = 12 \quad (6)$$

The *G* values for the minimized-E_{steric} conformers of reactants and products were first taken into account for the energy transition calculation, and the ΔE_{strain} values in the *O*-acylation reaction were similarly defined as the above equations (2)–(6).

The estimated in-reaction ΔG_e^{Tri} values were also significantly correlated as follows: (ΔG_e^{Tri}, X$_{aa}$) = (−97.34, Ala), (−139.79, Gly), and (−178.38, β-Ala) with square regression coefficient, $R^2 = 0.9942$ (Fig. 1a, open circles). As for the totally acylated models, the more significant correlation was obtained as, (ΔG_e^{TA}, X$_{aa}$) = (−763.43,

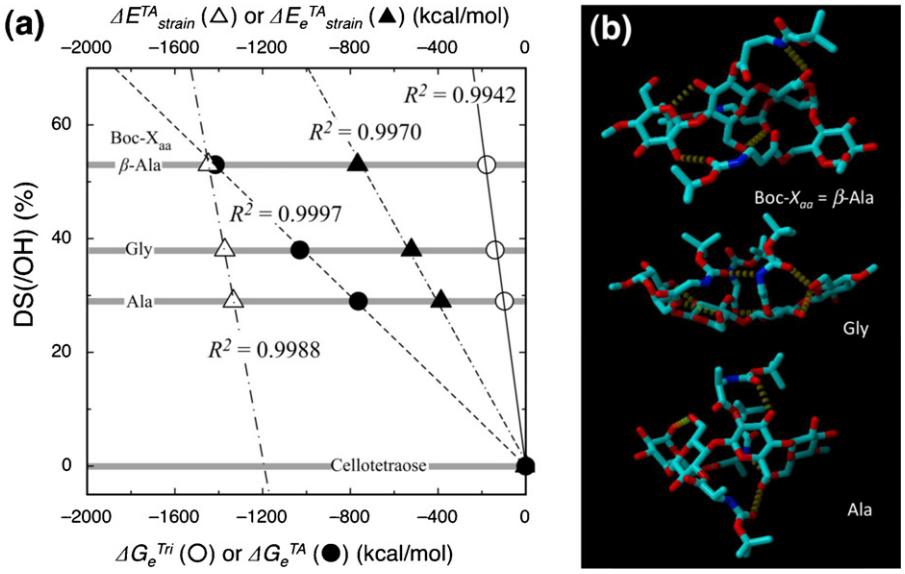

Fig. 1. (a) Correlation between the experimentally observed degree of substitution toward the cellulose hydroxyls (DS%(/OH)) and the calculated thermochemical parameters, ΔG_e^{Tri} (○, kcal/mol) and ΔG_e^{TA} (●, kcal/mol), and strain energy transitions, ΔE_{strain}^{TA} (□, kcal/mol) and $\Delta E_{e\,strain}^{TA}$ (▲, kcal/mol) (see text for definitions). (b) Molecular structures of the minimized-E_{steric} conformers.

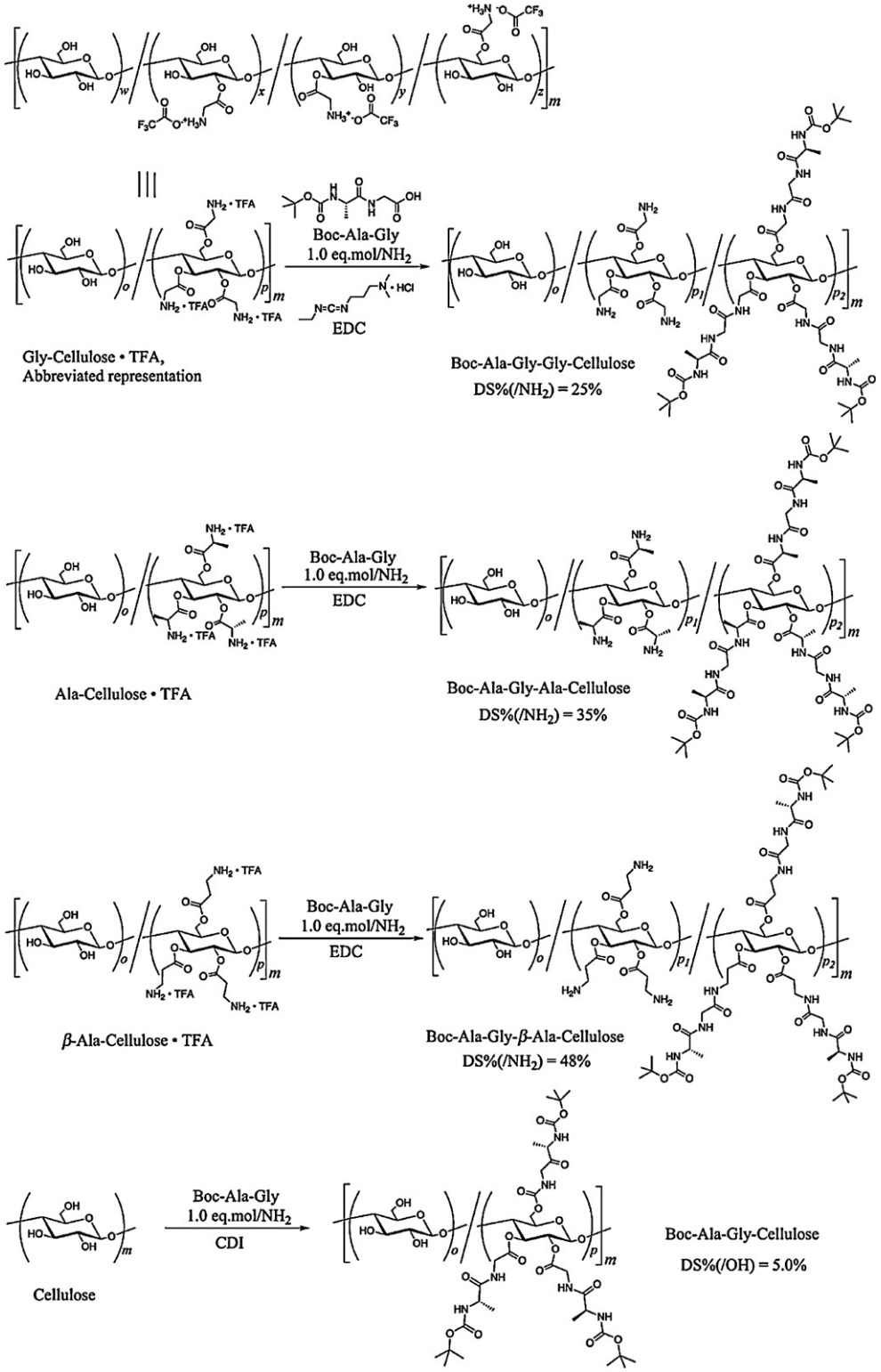

Scheme 2. Synthesis of Boc-Ala-Gly-X_{aa}-Celluloses *via* EDC-mediated *N*-acylation.

Ala), (−1030.24, Gly), and (−1415.61, β-Ala) with $R^2 = 0.9997$ (Fig. 1a, solid circles). These results clearly indicate that the *O*-acylation reactions of the parent cellulose molecules using Boc-X_{aa} and CDI are driven by the ΔG-based thermodynamic processes. The facts that the ΔE^{TA}_{strain} (Fig. 1a, open triangles) and $\Delta E^{TA}_{e\,strain}$ (Fig. 1a, solid triangles) exhibited $R^2 = 0.9988$ and $R^2 = 0.9970$, respectively, suggest that the highest steric freedom of β-Ala enables to release the greatest magnitude of the potential Gibbs's free energy, ΔG^{TA}, resulting in the largest *O*-acylation yield, *i.e.*, DS%(/OH) = 53% among three Boc-X_{aa}s.

The minimized-E_{steric} conformer distributions (CP, %) in the tri-*O*-acylated models were 61.44% and 61.58% for X_{aa} = Ala and

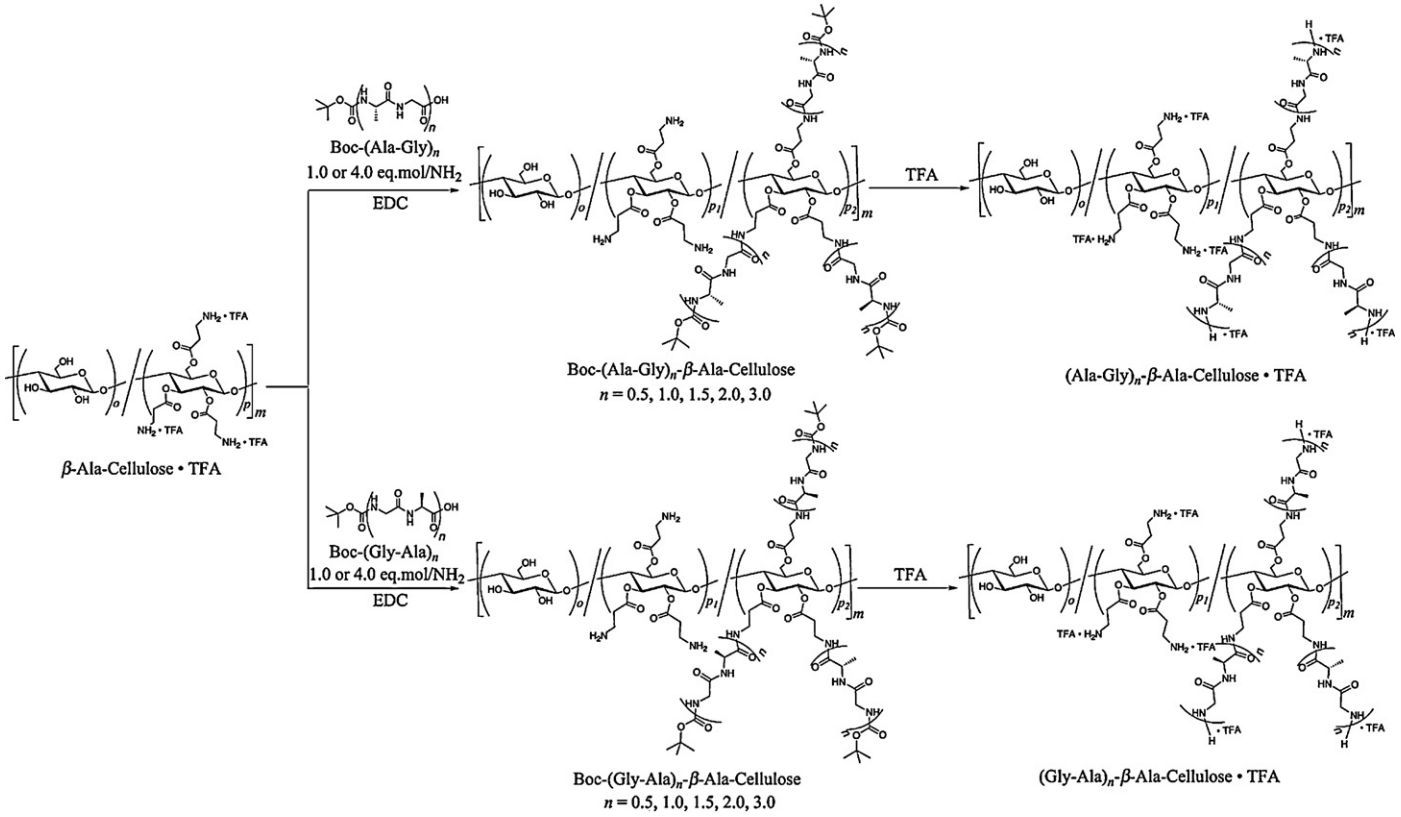

Scheme 3. Synthesis of Boc-(Ala-Gly)$_n$- and Boc-(Gly-Ala)$_n$-β-Ala-Celluloses *via* EDC-mediated *N*-acylation.

Gly, respectively, while in the case of X_{aa} = β-Ala, the CP value was 28.38%. The lower E_{steric} region in X_{aa} = β-Ala was in order from 100.70 kcal/mol (28.38%, minimum E_{steric}), 100.98 kcal/mol (20.01%), 101.12 kcal/mol (13.80%), and 101.31 kcal/mol (10.00%), indicating that the occupation of the lower E_{steric} conformers was 72.19% within 0.61 kcal/mol. These results indicated that the lower E_{steric} of the *O*-(Boc-β-Ala)-Cellulose was advantageous for promoting the *O*-acylation reaction due to adoption of relatively wide range of the side-chain conformations.

Fig. 1b represents the molecular models with the minimized-E_{steric} values for the *O*-(Boc-X_{aa})-cellotetraoses. For X_{aa} = Gly or Ala, the number of hydrogen bond (Hb)-free hydroxyls (-OH) on the parent cellulose was 2–3, much less than that of the *O*-(Boc-β-Ala)-cellotetraose having 5–6 Hb-free-OHs. The modeling result suggests that the Hb-free-OHs are responsible for the nucleophilic attack on the CDI-activated α-carbonyls during the *O*-acylation, resulting in the highest DS%(/OH) for the *O*-(Boc-β-Ala)-Cellulose.

3.2. *N*-Acylation of *O*-(X_{aa})-Cellulose using Boc-Ala-Gly

Removal of the Boc groups regenerated the primary amino groups to yield *O*-(X_{aa})-Cellulose TFA, which were subsequently subjected to the conjugation reactions with *N*-protected dipeptide, Boc-Ala-Gly, *via* selective *N*-acylation using EDC. In the "one-by-one" *N*-acylation (molar ratios, Boc-Ala-Gly: NH_2 of *O*-(X_{aa})-Cellulose = 1: 1), the DS%(/NH_2) value of *N*-(Boc-Ala-Gly)-β-Ala-Cellulose was the highest, DS%(/NH_2) = 48%, which means that approximately half of the fed dipeptide reacted with the amino group of *O*-(β-Ala)-Cellulose. The DS%(/NH_2) values for *N*-(Boc-Ala-Gly)-Gly-Cellulose and *N*-(Boc-Ala-Gly)-Ala-Cellulose were 25% and 31%, respectively (Scheme 2).

The *N*-acylation reaction of the *O*-(X_{aa})-Celluloses undergoes the formation of Boc-Ala-Gly anhydride, $(BocAG)_2O$, as a reactive intermediate to be α- (X_{aa} = Gly and Ala) or β-aminolyzed (X_{aa} = β-Ala) by the X_{aa}-Celluloses, of which model systems can be represented below:

$$m\,(\mathrm{BocAG})_2\mathrm{O} + O\text{-}(\mathrm{X_{aa}})\text{-cellotetraose} \rightarrow N\text{-}(2m\,\mathrm{BocAG})\text{-}\mathrm{X_{aa}}\text{-cellotetraose} \quad (7)$$

where the stoichiometry number was set in m = 1.5, which means that total *N*-acylation of tri-*O*-X_{aa}-acylated cellotetraose models, corresponding to each of the X_{aa}s in Scheme 2. The ΔG values are, thus, calculated by the Gibbs's free energy values of the reactants, $(BocAG)_2O$ and X_{aa}-cellotetraose, and the products, *N*-(Boc-Ala-Gly)-X_{aa}-cellotetraoses, which are obviously defined as $\Delta G = G_f - G_i$, and also for $\Delta E_{strain} = E_{strain,f} - E_{strain,i}$. The ΔG and ΔE_{strain} values were again concerned at first for the minimized-E_{steric} conformers.

Fig. 2a represents the correlation of the ΔG (kcal/mol) and DS%(/NH_2) (bottom axis, open circles), where the data sets were (ΔG, X_{aa}) = (18.42, Gly), (17.90, Ala), and (1.94, β-Ala) with R^2 = 0.9498 and for the strain energy transitions (top axis, in kcal/mol, solid circles), the calculated values were (ΔE_{strain}, X_{aa}) = (−6.25, Gly), (−17.72, Ala), and (−35.53, β-Ala) with R^2 = 0.9965 toward DS%(/NH_2). These results indicate that the *N*-acylations of X_{aa}-Celluloses are of the ΔG-driven thermodynamics, but the increased deviation (as seen in R^2 = 0.9498 for ΔG) implies the effect of the steric factors in more complicated structures of X_{aa}-Celluloses, as compared with $R^2 \geq 0.99$ in the *O*-acylation of the parent cellulose. The more significant correlation between ΔE_{strain} and DS%(/NH_2) in R^2 = 0.9965 also will support this consideration, and hence, the CP values and the lower-E_{steric} conformers of the *O*-(X_{aa})-cellotetraoses were inspected.

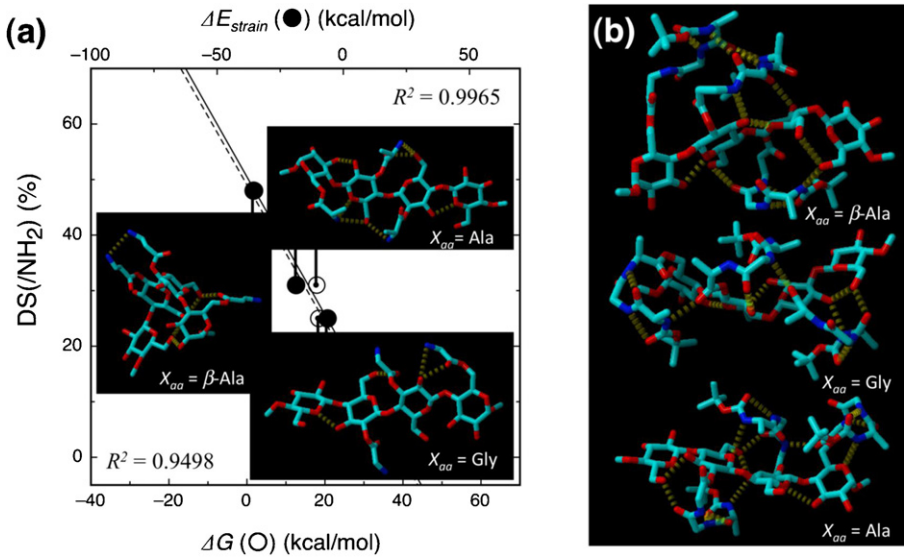

Fig. 2. (a) Correlation between the observed degree of substitution toward the NH_2 groups of *O*-(X_{aa})-Cellulose esters (DS%(/NH_2)) and the calculated ΔG (○, kcal/mol) and ΔE_{strain} (●, kcal/mol) (see text for definitions). Insets represent the minimized-E_{steric} conformers of the *O*-(X_{aa})-cellotetraose models. (b) The minimized-E_{steric} conformers of *N*-(Boc-Ala-Gly)-X_{aa}-cellotetraoses.

Fig. 2a insets show the molecular models of *O*-(X_{aa})-cellotetraoses having the minimized-E_{steric} values, and as for X_{aa} = Gly (CP = 32.24%) and Ala (CP = 30.80%), the cellotetraose backbone was likely extended as slightly twisted ribbons. Only when X_{aa} = β-Ala (CP = 19.34%), the cellotetraose backbone was strongly bent to form a helix-like geometry. These tendencies of the backbone adaptations were similar within the lowest 10-E_{steric} conformers, which covers total CP sums = 77.61% for X_{aa} = Gly, 83.12% for X_{aa} = Ala, and 61.30% for X_{aa} = β-Ala. Despite the bended backbone, *O*-(β-Ala)-cellotetraose is less strained with E_{strain} = 165.96 kcal/mol, as compared with others: (E_{strain}, X_{aa}) = (172.97, Gly) and (180.43, Ala) for the minimized-E_{steric} conformers. The number of Hb-free-NH_2 was 2 for X_{aa} = Gly, 0 for Ala, and 1 for β-Ala, while in the case of X_{aa} = β-Ala, absence of the Hbs between the β-NH_2 groups and the cellotetraose hydroxyls was characteristic, and this feature will promote the nucleophilic attack toward the symmetric anhydrides to yield more enhanced DS%(/NH_2) value.

Fig. 2b represents the minimized-E_{strain} models of the *N*-acylation products, *N*-(Boc-Ala-Gly)-X_{aa}-cellotetraoses. All of the three models have relatively extended backbones of the cellotetraoses, indicating that only in the case of X_{aa} = β-Ala, the *N*-acylation reconstituted the straightened backbone from the bent structure as seen in the pre-*N*-acylated conjugate model with relaxing the strain energy of the cellotetraose, as indicated by the calculated values of (E_{strain}, X_{aa}, CP) = (126.34, Gly, 66.39), (126.96, Ala, 78.42), and (121.58, β-Ala, 14.01) and the ΔE_{strain} values as previously mentioned. For X_{aa} = Gly and Ala, most of the *N*-substituents, *i.e.*, the *N*-(Boc-Ala-Gly)-moieties, adopted the β-turn-like peptide conformations and closely approached the cellotetraose backbones *via* multiple modes of Hbs without any of the inter-oligopeptide associations. On the other hand, in the case of X_{aa} = β-Ala, 2/3 of the *N*-substituents associated by means of β-strand formation, and in the force fields, tended to project from the backbone cellotetraose. The modeling results suggest that such a behavior of the *N*-(Boc-Ala-Gly)-β-Ala-moieties might gain the spatial freedom of the unreacted β-NH_2 groups, resulting in the greater extent of the *N*-acylation.

Since the direct *O*-acylation of the parent cellulose molecule using Boc-Ala-Gly resulted in the lowest DS%(/OH) of ~5.0% (Scheme 2), the *O*-(β-Ala)-Cellulose is conclusively the most preferable intermediate in the present examination for the two-step conjugate synthesis undergoing the *O*- and *N*-acylation reactions in turn.

3.3. Effect of peptide chain length on DS%(/NH_2) of *O*-(β-Ala)-Cellulose

The chain lengths of the Boc-oligo-peptides to be conjugated to *O*-(β-Ala)-Cellulose were represented as a variable *n* (repeating number), which has an increment unit of 0.5; for instance, in the case of Boc-(Gly-Ala)$_n$, *n* = 0.5 and 1.5 are identical to Boc-Gly and Boc-Gly-Ala-Gly, respectively (Scheme 3). The relationship between the repeating number *n* and the DS%(/NH_2) is represented in Fig. 3a. As for the Boc-(Ala-Gly)$_n$ series under the "one-by-one" condition for *N*-acylation (1.0 equiv.mol NH_2), the DS%(/NH_2) values increased from *n* = 0.5 (DS%(/NH_2) = 35%) to *n* = 1.5, at which the DS%(/NH_2) was maximum (91%), then decreased toward *n* = 3 (DS%(/NH_2) = 59%), indicating the presence of a suitable chain length for the higher *N*-acylation yield.

The *N*-acylation reactions of tri-*O*-acylated β-Ala-cellotetraose using the Boc-oligo-peptides can be represented as follows:

$$m\,(\mathrm{Boc(AG)}_n)_2\mathrm{O} + O\text{-}(\beta\text{-Ala})\text{-cellotetraose} \rightarrow N\text{-}(2m\,\mathrm{Boc(AG)}_n)\text{-}\beta\text{-Ala-cellotetraose} \quad (8\text{-}1)$$

and

$$m\,(\mathrm{Boc(GA)}_n)_2\mathrm{O} + O\text{-}(\beta\text{-Ala})\text{-cellotetraose} \rightarrow N\text{-}(2m\,\mathrm{Boc(GA)}_n)\text{-}\beta\text{-Ala-cellotetraose} \quad (8\text{-}2)$$

where the stoichiometry number was similarly set in *m* = 1.5, and the symbols, (Boc(AG)$_n$)$_2$O and (Boc(GA)$_n$)$_2$O, are the corresponding anhydrides of the Boc-oligo-peptides. The DS%(/NH_2)-weighted free energy transition, ΔG_e (kcal/mol), was calculated for the minimized-E_{steric} conformers of the acylating agents (anhydrides), β-Ala-cellotetraose, and the product conjugates; however, the resulting ΔG_e values not clearly correlated toward the observed DS%(/NH_2), where for Boc-(Ala-Gly)$_n$ series, (n, ΔG_e) = (0.5, 5.33), (1.0, 1.04), (1.5, 7.62), (2.0, 12.76), and (3.0, 5.66) with R^2 = 0.3578, and for Boc-(Gly-Ala)$_n$ series, (n, ΔG_e) = (0.5, 1.69), (1.0, 0.917), (1.5,

33.30), (2.0, 14.78), and (3.0, 6.18) with $R^2 = 0.6214$. Similarly, the DS%(/NH_2)-weighted strain energy transition, $\Delta E_{e,strain}$ (kcal/mol) was also calculated for the minimized-E_{steric} conformers of the reactants, but no significant correlation was observed. These results suggest that, in the case of the *N*-acylation using Boc-oligo-peptide, several steric factors of the *N*-acylating agents involved affects to yield the product conjugate with higher DS%(/NH_2), besides the ΔG-based thermodynamics.

Fig. 3b left column represents the cross-point stereograms of all models built for the minimized-E_{steric} symmetric anhydrides using

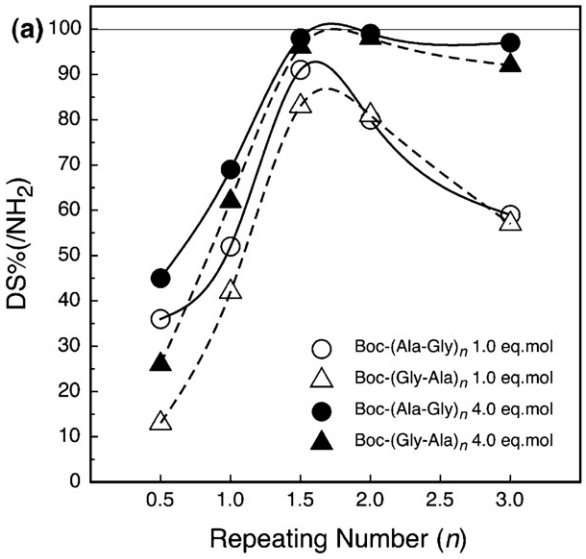

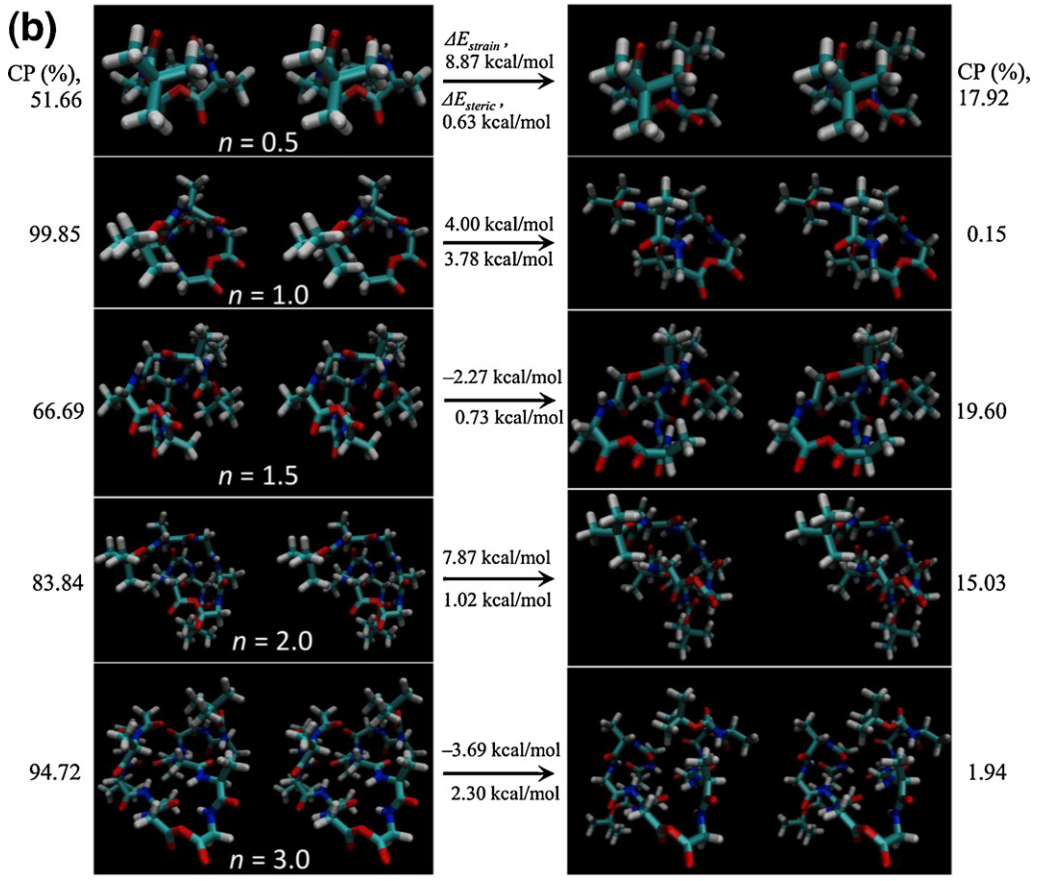

Fig. 3. (a) Relationship between the observed DS%(/NH_2) and the repeat numbers (n, 0.5, 1.0, 1.5, 2.0, and 3.0) of Boc-(Ala-Gly)$_n$ and Boc-(Gly-Ala)$_n$, which were used for *N*-acylation reactions of the *O*-(*β*-Ala)-Cellulose. Cross-point stereograms of the symmetric anhydrides of (b) Boc-(Ala-Gly)$_n$ and (c) Boc-(Gly-Ala)$_n$ as reactive intermediates in the *N*-acylation reactions. Left columns, the minimized-E_{steric} conformers having the lowest E_{steric}. Right columns, the second minimized-E_{steric} conformers having the second-lowest E_{steric}. Arrows with numbers between columns, strain and steric energy transitions from the minimized-E_{steric} to the second minimized-E_{steric} conformers. CP (%), conformer populations in percentages.

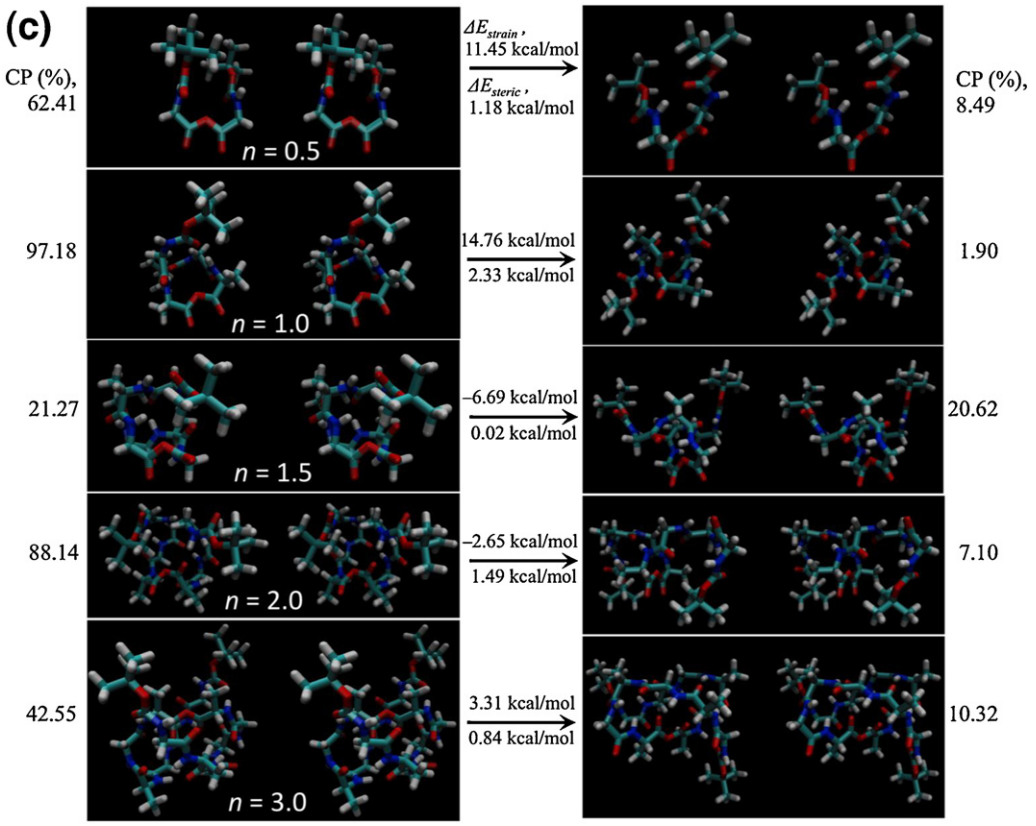

Fig. 3. (*Continued*).

the VMD version 1.91 software (Humphrey, Dalke, & Schulten, 1996). As for the anhydrides having $n = 0.5$ and 1.0, the anhydride moieties of both models arranged in the most stable plane, but the steric hindrance over the n-π orbitals in the $n = 1.0$-model is reduced as compared to that of the $n = 0.5$-model. The $n = 0.5$- and 1.0-models occupied 51.66 and 99.85% of CPs, respectively, and the transition energies to the second minimized-E_{steric} conformers (Fig. 3b, right column) were (ΔE_{steric}, ΔE_{strain}) = (8.87, 0.63) for the $n = 0.5$-model (CP, 19.72%) and (4.00, 3.78) for the $n = 1.0$-model (CP, 0.15%). One side of the n-π orbital plane in the $n = 2.0$-model is slightly torsional and exposed to the bulk, which allows a more frequent aminolysis by the *O*-(β-Ala)-Cellulose. These properties become most remarkable in the $n = 1.5$-model for which the DS%(/NH_2) was highest at 91%. The anhydride torsion of the first minimized-E_{steric} conformer (CP, 66.69%) was retained during the conformational transition to the second minimized-E_{steric} conformer (CP, 19.60%), for which (ΔE_{steric}, ΔE_{strain}) was (0.73, −2.27). In the case of the $n = 3.0$-model, the tightly associated two hexapeptide moieties almost completely block one side of the n-π orbital plane with a lower magnitude of torsion.

A similar argument was adopted for the *N*-acylation using the Boc-(Gly-Ala)$_n$ series; only the $n = 1.5$- and 2.0-models exhibited the tendencies in the conformational characteristics similar to the $n = 1.5$-model of the Boc-(Ala-Gly)$_n$. The transition to the second minimized-E_{steric} conformer involved (ΔE_{steric}, ΔE_{strain}) = (0.02, −6.69) for the $n = 1.5$-model (CP, 20.62%) and (1.49, −2.65) for the $n = 2.0$ model (CP, 7.10%) (Fig. 3c), for which the DS%(/NH_2) were observed as the highest yields of the *N*-acylation, 81–83%. Commonly in the Boc-(Ala-Gly)$_n$ and Boc-(Gly-Ala)$_n$ series, the $n = 1.5$-models of the symmetric anhydride exhibited the most wide extent of the CP distributions, the values of which were, from the first minimized-E_{steric} conformer, CP = 66.69, 19.60, 3.40, 3.31, and 1.55% toward the 5th-minimized-E_{steric} conformer for the Boc-(Ala-Gly)$_n$ series, and in the case of the Boc-(Gly-Ala)$_n$ series, CP = 21.27, 20.62, 16.64, 9.51, and 6.11%. These modeling results strongly suggested that the structural features, including the steric hindrance and the torsional energy of the reactive symmetric anhydride, affect the degree of *N*-acylation.

3.4. Solubility tests

As for the Boc-(Ala-Gly)$_n$ and Boc-(Gly-Ala)$_n$ conjugate series, their solubility in distilled water (DW) is significantly different from each other; Boc-(Ala-Gly)$_n$ series was soluble in DW for all tested n values, while the Boc-(Gly-Ala)$_n$ series was not, except for $n = 1$ (Table 1). The Boc-(Ala-Gly)$_n$ conjugates ($n = 1.0$–2.0) swelled or dissolved in methanol, on the other hand, the Boc-(Gly-Ala)$_n$ conjugates were only swollen in methanol for $n = 1$ and insoluble for $n = 1.5$–3.0. This observation implies that the repeat –Gly-Ala– expresses a stronger aggregation force among the conjugate molecules, as compared with the –Ala-Gly– repeats. The fact that the *N*-[Boc-(Gly-Ala)$_n$]-β-Ala conjugates ($n = 1.0$–1.5) were always prepared with the lower DS%(/NH_2) as compared to the Boc-(Ala-Gly)$_n$ series was probably due to the relatively enhanced aggregating properties.

Regeneration of the *N*-end amino groups altered the solubilities of both the Boc-(Ala-Gly)$_n$ and Boc-(Gly-Ala)$_n$ conjugates; as for $n = 1.0$–1.5, the former conjugates were swollen in DW, while the latter conjugates were insoluble, and for $n = 2.0$–3.0, both conjugates were soluble in water and swollen in methanol, but insoluble in acetone and dioxane. These results suggest that the distal ends of the two dipeptide units having a TFA·NH_2-salt may be hydrated to allow contact between H_2O molecules and the more proximal moiety of the *N*-linked peptides, resulting in dissolution of the

Table 1
Solubility tests in various solvents.

	Repeating number (n)	Solvents						
		DW	MeOH	$(Me)_2CO$	$CHCl_3$	$(EtO)_2$	C_6H_6	DMSO
Boc-(Ala-Gly)$_n$	1.0	S[a]	SW[b]	SW	SW	SW	S	S
	1.5	S	S	IS[c]	SW	IS	SW	S
	2.0	S	S	IS	SW	IS	SW	S
	3.0	S	IS	IS	SW	SW	SW	S
Boc-(Gly-Ala)$_n$	1.0	S	SW	SW	SW	SW	SW	S
	1.5	IS	IS	IS	SW	IS	SW	S
	2.0	IS	IS	SW	SW	SW	SW	S
	3.0	IS	IS	IS	SW	SW	SW	S
TFA (Ala-Gly)$_n$	1.0	SW	IS	IS	IS	IS	SW	S
	1.5	SW	IS	IS	IS	IS	SW	S
	2.0	S	SW	IS	SW	IS	SW	S
	3.0	S	SW	IS	SW	IS	SW	S
TFA (Gly-Ala)$_n$	1.0	IS	IS	IS	IS	IS	SW	S
	1.5	IS	IS	IS	SW	IS	SW	S
	2.0	S	SW	IS	SW	IS	SW	S
	3.0	S	SW	IS	SW	IS	SW	S

[a] Soluble (at 2.0 mg/100 μL).
[b] Swollen.
[c] Insoluble.

conjugate molecule. DMSO was able to solubilize all of the conjugate molecules tested. In summary, the solubility test indicated that both the sequence and chain length of the conjugated peptide can modify the interaction especially with the polar solvents.

4. Conclusion

The present study proposed several insights into the origin of the reactive properties of the *O*-(*β*-Ala)-Cellulose as follows: (i) during the *O*-acylation step, the *O*-linked Boc-*β*-Ala residue tends to extend away from the parent cellulose molecule with moderate twisting of the polysaccharide chains, resulting in preservation of the greater number of Hb-free hydroxyls, which are available for alcoholysis of the activated *α*-carbonyls bound to imidazole, as well as releasing approximately 53% of the theoretical steric energy potential based on the ΔG_e- and ΔE_{strain}-based prediction by the total *O*-acylation model and also the experimental observations of DS%(/OH); (ii) after removal of the Boc-groups, the *O*-linked *β*-Ala residues further bend the parent molecular backbone to acquire the greater magnitude of the strain potential, and during the *N*-acylation step, the *β*-Ala residues allow the *N*-linked Boc-Ala-Gly moiety to project toward the bulk, along with re-extending the parent molecular backbone, the process of which can release ΔE_{strain} by −35.53 kcal/mol for the theoretical strain energy potential.

In the *N*-acylation using series of the protected oligo-peptides, Boc-(Ala-Gly)$_n$ and Boc-(Gly-Ala)$_n$, the conformational characteristics of the symmetric anhydrides as the *N*-acylating agents indicated that, especially for the $n = 1.5$-anhydrides, the steric stabilization of the peptide moiety *via* the *β*-like-paired-strands association was coupled with the torsional destabilization of the anhydride moiety. The breakdown of such types of anhydrides *via* the aminolysis by *O*-(*β*-Ala)-Cellulose, together with the effect (ii), will promote the *N*-acylation reaction to yield the highly substituted product having DS%(/NH_2) = 81–91%. The $n \geq 2$-models, depending on their sequence types, have inherent degrees of drawbacks as the steric hindrance of the anhydride moiety due to the longer peptide chains.

In order to increase the DS%(/NH_2), one possible way is to feed greater amounts of the protected peptides for the *N*-acylation reaction. As experimentally observed, at a 4.0-equiv.mol NH_2 condition, the *N*-acylation of the *O*-(*β*-Ala)-Cellulose using the Boc-(Ala-Gly)$_n$ series having $n \geq 1.5$ yielded almost saturated DS%(/NH_2) values of 97–98%, which means that a ca. 3-fold- molar excess of the synthetic peptides were lost unreacted. A more promising procedure will be to alter the coupling chemistry for the *N*-acylation, *e.g.*, our previous observations indicated that the use of isobutyl chloroformate resulted in a higher DS%(/NH_2) of 68–97% in which the stoichiometry was 1:1.2 between the *β*-NH_2 groups of *O*-(*β*-Ala)-Cellulose and the protected peptide having more complex chemical structures involving the *O*-phosphorylated-serines (Devarayan et al., 2013).

In conclusion, the *O*-(*β*-Ala)-Cellulose possesses the preferable properties for synthesizing the peptide–cellulose conjugate in a homogenous reaction system, which is similar to the liquid-phase coupling procedures often used in the peptide synthesis. The *C*-end-on synthesis for *O*-acylation of the parent cellulose using Boc-*β*-Ala as the first step and *N*-acylation of the regenerated *β*-amino groups using the given protected oligo-peptides as the second step can be adopted for one of the multipurpose cellulose conjugate syntheses, of which function can be brought by the peptides moieties bound to the *β*-amino groups.

The chemical reactivity of cellulose, including the *O*-acylation regio-selectivity, has been characterized using a numerical simulation (Salmi, Damlin, Mikkola, & Kangas, 2011), on the other hand, the reactivity predictions of the cellulose derivatives using molecular mechanics/dynamics combined with thermochemical computations are still remained to be established. The present simple models for energy profile analysis, *i.e.*, cellotetraose derivatives and acylating agents both of which are generated by the conformer search calculation, mostly can be correlated with the observed results. In order to improve the accuracy of the present predictions, as previously described on the *O*-6-oriented/random parallel substitution of the Boc-*β*-Ala-Cellulose which was determined by quantitative NMR spectroscopy (Devarayan et al., 2013), more complicated but precise modeling will be required for computations.

Acknowledgments

This work was supported by Grants in Aid No. 22350103 and No. 23651083, and in part by the Grant in Aid for Global COE Program by the Ministry of Education, Culture, Sports, Science, and Technology, Japan. Part of this study was performed through the Program for Dissemination of Tenure-Track System funded by the Ministry of Education and Science, Japan.

Appendix A. Supplementary data

Supplementary data associated with this article can be found, in the online version, at http://dx.doi.org/10.1016/j.carbpol.2012.12.074.

References

Adler, S., Frank, R., Lanzavecchia, A., & Weiss, S. (1994). T cell epitope analysis with peptides simultaneously synthesized on cellulose membranes: Fine mapping of two DQ dependent epitopes. *FEBS Letters*, *352*, 167–170.

Burkert, U., & Allinger, N. L. (1982). *Molecular mechanics, ACS monograph 177*. Washington, DC: American Chemical Society. (Chapter 5)

Devarayan, K., Hachisu, M., Araki, J., & Ohkawa, K. (2013). Synthesis of peptide–cellulose conjugate mediated by a soluble cellulose derivative having β-Ala esters (II): Conjugates with O-phospho-L-serine-containing peptides. *Cellulose*, *20*, 365–378. http://dx.doi.org/10.1007/s10570-012-9822-1

Frank, R., & Doring, R. (1988). Simultaneous multiple peptide synthesis under continuous flow conditions of cellulose paper discs as segmental solid supports. *Tetrahedron*, *44*, 6031–6040.

Frisch, M. J., Trucks, G. W., Schlegel, H. B., Scuseria, G. E., Robb, M. A., Cheeseman, J. R., et al. (2009). *Gaussian 09, revision A.1*. Wallingford CT: Gaussian, Inc.

Gardner, T. S. (1946). Cellulose acetate esters containing amino nitrogen. *Journal of Polymer Science*, *1*, 121–126.

Goto, H., & Osawa, E. (1989). Corner flapping: A simple and fast algorithm for exhaustive generation of ring conformations. *Journal of the American Chemical Society*, *111*, 8950–8951.

Goto, H., & Osawa, E. (1993). An efficient algorithm for searching low-energy conformers of cyclic and acyclic molecules. *Journal of the Chemical Society, Perkin Transactions*, *2*, 187–198.

Halgren, T. A. (1999). MMFF VI. MMFF94s option for energy minimization studies. *Journal of Computational Chemistry*, *20*, 720–729.

Hanwell, M., Curtis, D., Lonie, D., Vandermeersch, T., Zurek, E., & Hutchison, G. (2012). Avogadro: An advanced semantic chemical editor, visualization, and analysis platform. *Journal of Cheminformatics*, *4*, 17.

Hayakawa, D., Ueda, K., Yamane, C., Miyamoto, H., & Horii, F. (2011). Molecular dynamics simulation of the dissolution process of a cellulose triacetate-II nanosized crystal in DMSO. *Carbohydrate Research*, *346*, 2940–2947.

Heinze, T., & Liebert, T. (2001). Unconventional methods in cellulose functionalization. *Progress in Polymer Science*, *26*, 1689–1762.

Humphrey, W., Dalke, A., & Schulten, K. (1996). VMD: Visual molecular dynamics. *Journal of Molecular Graphics*, *14*, 33–38.

Kramer, A., Reineke, U., Dong, L., Hoffmann, B., Hoffmuller, U., Winkler, D., et al. (1999). Spot synthesis: Observations and optimizations. *Journal of Peptide Research*, *54*, 319–327.

Kuboe, Y., Tonegawa, H., Ohkawa, K., & Yamamoto, H. (2004). Quinone cross-linked polysaccharide hybrid fiber. *Biomacromolecules*, *5*, 348–357.

Liebert, T., & Heinze, T. (2005). Tailored cellulose esters: Synthesis and structure determination. *Biomacromolecules*, *6*, 333–340.

Luo, N., Stewart, M. J., Hirt, D. E., Husson, S. M., & Schwark, D. W. (2004). Surface modification of ethylene-co-acrylic acid copolymer films: Addition of amide groups by covalently bonded amino acid intermediates. *Journal of Applied Polymer Science*, *92*, 1688–1694.

Mazeau, K., & Charlier, L. (2012). The molecular basis of the adsorption of xylans on cellulose surface. *Cellulose*, *19*, 337–349.

Ohkawa, K., Nishida, A., Yamamoto, H., & Waite, J. H. (2004). A glycosylated byssal precursor protein from the green mussel *Perna viridis* with modified dopa sidechains. *Biofouling*, *20*, 101–115.

Ohkawa, K., Nishibayashi, M., Devarayan, K., Hachisu, M., & Araki, J. (2013). Synthesis of peptide-cellulose conjugate mediated by a soluble cellulose derivative having *β*-Ala esters. *International Journal of Biological Macromolecules*, *53*, 150–159.

Queyroy, S., Muller-Plathe, F., & Brown, D. (2004). Molecular dynamics simulations of cellulose oligomers: Conformational analysis. *Macromolecular Theory and Simulations*, *13*, 427–440.

Salmi, T., Damlin, P., Mikkola, J. P., & Kangas, M. (2011). Modelling and experimental verification of cellulose substitution kinetics. *Chemical Engineering Science*, *66*, 171–182.

Sato, T., Karatsu, K., Kitamura, H., & Ohno, Y. (1983). Synthesis of cellulose derivatives containing amino acid residues and their adsorption of metal ions. *Sen'i Gakkaishi*, *39*, T519–T524.

Stewart, J. P. (2007). Optimization of parameters for semiempirical methods V: Modification of NDDO approximations and application to 70 elements. *Journal of Molecular Modeling*, *13*, 1173–1213.

Sun, T., Derevitskaya, V. A., & Rogovin, Z. A. (1959). Structure and properties of cellulose and its esters. LXXXII. Synthesis of new derivatives of cellulose and other polysaccharides. II. Synthesis of amides of alginic acid and carboxymethylcellulose with amino acids. *Vysokomolekulyarnye Soedineniya*, *1*, 1178–1181.

Tonegawa, H., Kuboe, Y., Amaike, M., Nishida, A., Ohkawa, K., & Yamamoto, H. (2004). Synthesis of enzymatically crosslinkable peptide-poly(L-lysine) conjugate and creation of bio-inspired hybrid fibers. *Macromolecular Bioscience*, *4*, 503–511.

Winkler, D. F. H. (2011). Chemistry of SPOT synthesis for the preparation of peptide macroarrays on cellulose membranes. *Mini-Reviews in Organic Chemistry*, *8*, 114–120.

Yamamoto, H., Saitoh, A., & Ohkawa, K. (2003). Synthesis of sequential polypeptides containing *O*-phospho-L-serine. *Macromolecular Bioscience*, *7*, 354–363.

Yanagisawa, M., Shibata, I., & Isogai, A. (2004). SEC-MALLS analysis of cellulose using LiCl/1,3-dimethyl-2-imidazolidinone as an eluent. *Cellulose*, *11*, 169–176.

Yoshida, Y., Isogai, A., & Tsujii, Y. (2008). Structural analysis of polymer-brush-type cellulose beta-ketoesters by molecular dynamics simulation. *Cellulose*, *15*, 651–658.

Yui, T., Nishimura, S., Akiba, S., & Hayashi, S. (2006). Swelling behavior of the cellulose I beta crystal models by molecular dynamics. *Carbohydrate Research*, *341*, 2521–2530.

Zarth, C. S. P., Koschella, A., Pfeifer, A., Dorn, S., & Heinze, T. (2011). Synthesis and characterization of novel amino cellulose esters. *Cellulose*, *18*, 1315–1325.